

# **Physical and Mechanical Properties of a Porous Material obtained by low Replacement of Volcanic Ash by Aluminum Beverage Cans**

---

## **ABSTRACT**

This study focuses on the evaluation of the physical and mechanical properties of a porous material based on a mixture of powder (Volcanic ash /Aluminum Beverage Cans) and a solution of phosphoric acid. Volcanic ash (VA) use was collected in one of the quarries of Mandjo (Cameroon coastal region), crushed, then characterized by XRF, DRX, FTIR and named MaJ. The various polymers obtained are called MaJ<sub>0</sub>, MaJ<sub>2.5</sub>, MaJ<sub>5</sub>, MaJ<sub>7.5</sub> and MaJ<sub>10</sub> according to the mass content of the additions of the powder from the aluminum beverage cans (ABCs). The physical and mechanical properties of the synthetic products were evaluated by determining the apparent porosity, bulk density, water absorption and compressive strength. The results of this study show that the partial replacement of the powder of VA by that of ABC leads to a reduction in the compressive strength (5.9 - 0.8 MPa) and bulk density (2.56 – 1.32 g/cm<sup>3</sup>) of the polymers obtained. On the other hand, apparent porosity, water absorption and pore formation within the polymers increases with addition of the powder from the beverage cans. All of these results allow us to agree that the ABCs powder can be used as a blowing agent during the synthesis of phosphate inorganic polymers.

*Keywords: Mechanical properties, porous material, volcanic ash, aluminum beverage cans, phosphoric acid*

## **1. INTRODUCTION**

Volcanic ash (VA) are fragments of pulverized rocks, minerals or crystals and volcanic glass shards obtained during volcanic eruption and usually having a diameter less than 2mm [1-4]. Djobo et al [2] report that according to their morphologies, VA can be classified into two large families, namely pumice and slag. They also report that VA are used in agriculture as a conditioner to increase soil porosity, abrasives, absorbents, ceramics and construction. In Cameroon, this rock debris constitutes fairly significant quarries visible along the Cameroonian volcanic line (around 1600 km) and is more used in the construction sector. In that domain, they are mostly used as lightweight aggregates in concrete, pozzolan for making blended cement and for road improvement. VA can also be used as fillers [5] or raw

material for the preparation of geopolymer binders [2-4]. It is important to mention that this aluminosilicate source can also be used in other fields such as water treatment [6]. On the other hands, for several years, the brewing industry has produced different types of beverages which are usually stored in various types of packaging (glasses, P.E.T and aluminum beverage can). In Cameroon, after the inauguration on February 19, 2018 of a new bottling line for the packaging of beers in cans and in order to fight against fraud of its various soft drinks imported from neighboring countries, the Cameroonian brewing industry (Société Anonyme des Brasseries du Cameroun (SABC)) has set up a production chain for ABCs [7]. The production capacity of this new chain is 16,000 cans per hour for 33 cl drinks and 12,000 for 50 cl drinks. However, after use, these cans are dumped in landfills and participate in the pollution of our environment. Although in Cameroon the recycling of this waste has not yet materialized, according to <http://recycling.world-aluminium.org/regional-reports/brazil/> [8] Brazil recycles 98.4%. Thus, the revalorization of this waste by geopolymerization can be of a major advantage in our social environment. It is important to note that, the aluminum beverage cans from the brewing product production units are essentially made of aluminum (around 97.5%) [9] and therefore, the waste obtained after use can be used as a blowing agent during the development of porous inorganic polymers. Indeed, several studies have shown that the use of an additional source of silicon or aluminum during the synthesis of inorganic polymers promotes the formation of pores within the synthetic products obtained [10-14]. For example Hamed et al [13] show that the use of inorganic polymers rich in Al and Fe during the synthesis of sesame-based activated carbons leads to a modification of the structural properties and morphology of the materials. The authors claim that the presence of aluminium and iron in the activated carbon matrix is responsible for the increase in pore volume and absorption capacity. This point of view is also shared by Hertel et al [14] show that, with an increase amount of aluminum and L/S ratio, more H<sub>2</sub> is generate which leads to an increase porosity of bauxite residue-based porous inorganic polymer. This study focuses on the evaluation of the physical and mechanical properties of porous inorganic polymers obtained by partial replacement of VA by powder of ABCs from the Cameroonian brewing industries by the sol-gel method. The aluminosilicate raw material was characterized by XRF, XRD and FTIR. The physical and mechanical properties of porous inorganic polymers will be evaluated by determining the apparent porosity, water absorption, bulk density and compressive strength.

## **2. MATERIAL AND EXPERIMENTAL METHODS**

### **2.1 Materials**

VA used in this study was collected from department of Mounjo in the locality of Manjo (Cameroon coastal region). The geographic coordinates of the harvesting areas are  $4^{\circ} 51'47.1780''$  North latitude and  $9^{\circ} 50'18.6360''$  East longitude. The harvested rock blocks were dried at  $110^{\circ}\text{C}$  for 24 hours to facilitate grinding. Then, it was ground in a ball mill with a porcelain pot for a period of 6 hours and finally sieved to obtain particles of size less than  $125\ \mu\text{m}$  and was called MaJ. The aluminum beverage cans were picked up at various landfills in the city of Douala (Littoral-Cameroon). The procedure for obtaining powder of ABCs is identical to that used for MaJ. Fig1 shows the images of these two materials before and after grinding.



**Fig 1.** Image of the raw materials before and after the grinding

The acid activator solution was prepared by dilution in distilled water, a commercial solution of orthophosphoric acid ( $\text{H}_3\text{PO}_4$ ) with a purity of 85 %. At the end of this dilution, we obtained a daughter solution of 4M molarity and whose  $\text{P}_2\text{O}_5 / \text{H}_2\text{O}$  ratio percentage is equal to 2.4. This solution will be left to stand for a minimum of 24 hours in order to facilitate the depolymerization of orthophosphoric acid and to better promote the polycondensation step in this geopolymerization process.

## **2.2 Preparation of porous materials**

The porous materials was obtained by mixing VA / ABCs powder to an activating solution of 4M molarity according to a L/S mass ratio equal to 0.45. The whole is mixed in an electric mixer of the PHILLIPS brand for a period of 2 Min, until a homogeneous paste is obtained. The fresh paste obtained will be poured into two types of cylindrical and cubic PVC test pieces ( $D = 20\text{mm}$ ,  $h = 40\text{mm}$  and  $20 \times 20 \times 20\text{mm}$ ) and put under vibration for 5 Min, then kept in a corner of the laboratory for 24 hours before being demolded. After release from the

mold, five formulations called MaJ<sub>0</sub>, MaJ<sub>2.5</sub>, MaJ<sub>5</sub>, MaJ<sub>7.5</sub> and MaJ<sub>10</sub> are obtained according to the mass percentage of addition of ABCs powder whose compositions are listed in Table1.

**Table 1.** Mix proportions design for porous materials

Mixture	Replacement level of VA by ABC (g)	VA (g)	ABC/VA	L/S
MaJ <sub>0</sub>	0	100	0	0.45
MaJ <sub>2.5</sub>	2.5	97.5	0.026	0.45
MaJ <sub>5.0</sub>	5.0	95.0	0.052	0.45
MaJ <sub>7.5</sub>	7.5	92.5	0.081	0.45
MaJ <sub>10</sub>	10.0	90.0	0.110	0.45

These different specimens will be kept safe from contamination for 28 days before being subjected to physical and mechanical tests. Fig 2 summarizes the experimental protocol for the synthesis of the different samples.

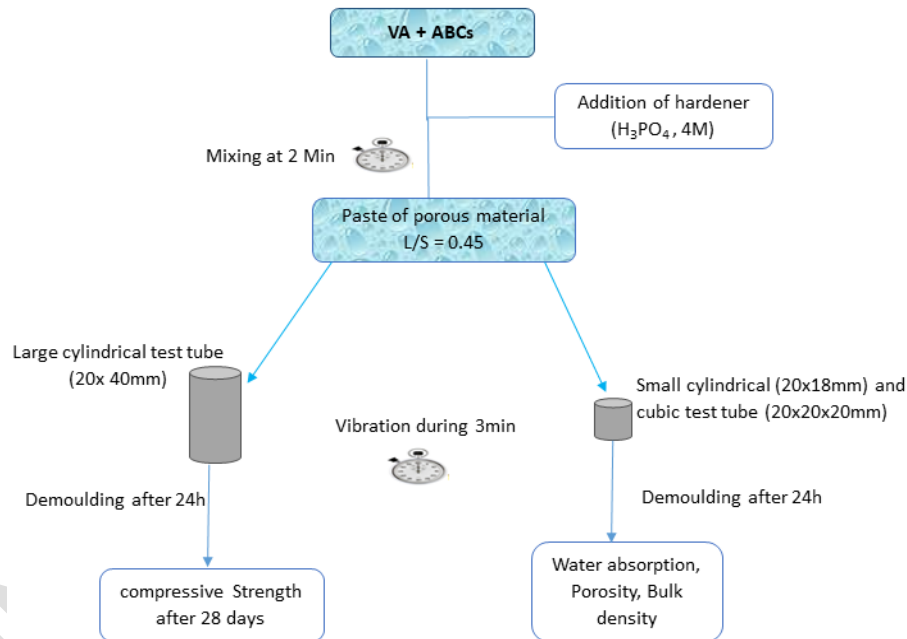


**Fig 2.** Experimental procedure for the synthesis of porous material

### 2.3 Analytical Methods

The chemical composition of the volcanic ash determined with fluorescence by X-Ray is given in Table2. Its mineralogical composition determination of was done thanks to a Bruker D2 Phaser which operated using  $K\alpha$  radiation of copper ( $\lambda = 1,54184 \text{ \AA}$ ) in the range of  $5\text{--}50^\circ$  ( $2\theta$ ) and crystalline phases were identified by comparing the obtained

patterns with the Powder Diffraction File (PDF) standards from the International Centre for Diffraction Data (ICDD). Thermo Scientific Nicolet IS 5 was the FTIR Spectrometer device which operated at ATR mode on a germanium crystal for the characterization of various samples in transmittance mode. Measurements were recorded in the range of 4000 and 400  $\text{cm}^{-1}$ .

**Table 2.** Chemical composition of raw materials and phosphoric acid.

Oxides	SiO <sub>2</sub>	Al <sub>2</sub> O <sub>3</sub>	Fe <sub>2</sub> O <sub>3</sub>	CaO	MgO	TiO <sub>2</sub>	Na <sub>2</sub> O	K <sub>2</sub> O	P <sub>2</sub> O <sub>5</sub>	LOI
MaJ	41.52	15.90	14.74	9.67	8.29	3.45	2.30	0.63	0.75	2.44
H <sub>3</sub> PO <sub>4</sub>	-	-	-	-	-	-	-	-	85.00	-

The mechanical properties was investigate by compressive strength of the synthesized product aged of 28 days. Apparatus using an electrohydraulic press with capacity of 60 KN (M & O, type 11.50, N ° 21) refer to ASTM C 109 Standard. The final values was average of four tested specimens. On the other hand, for the physicochemical properties, the water absorption test, apparent porosity and bulk density of porous materials was determined according to the norm ASTM C-20 [15].

### 3. RESULTS AND DISCUSSION

#### 3.1 Characterization of VA

The results of the chemical composition of MaJ are given in Table2. It appears that the VA used mainly contain SiO<sub>2</sub>, Al<sub>2</sub>O<sub>3</sub>, Fe<sub>2</sub>O<sub>3</sub>, CaO and MgO. Added that, are low contents of Na<sub>2</sub>O (2.3 %wt) and TiO<sub>2</sub> (3.45 %wt). Moreover, a content of CaO (9.67 %wt) and MgO (8.29 %wt) oxides present in MaJ, can intervene and lead to a possible modification of the structure of the polymeric network [16].

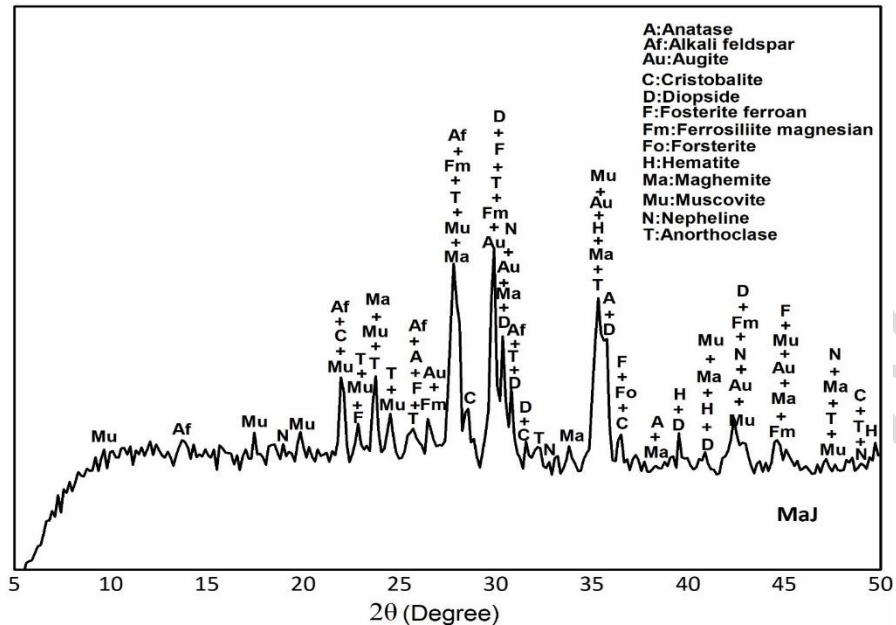


**Fig 3.** XRD Pattern of volcanic ash

On the other hand, the X-ray pattern of MaJ (Fig.3) reveals the presence of many crystalline phases such as Anatase [TiO<sub>2</sub>, PDF:75-1537], Anorthoclase [(Na,K)(Si<sub>3</sub>Al)O<sub>8</sub>, PDF:09-0478], Augite [Ca(Mg<sub>0.85</sub>Al<sub>0.15</sub>)(Si<sub>1.70</sub>Al<sub>0.30</sub>)O<sub>6</sub>, PDF:78-1391], Cristobalite [SiO<sub>2</sub>, PDF:89-3434], Diopside aluminian [Ca(Mg,Fe,Al)(Si,Al)<sub>2</sub>O<sub>6</sub>, PDF:38-0466], Feldspar [Na(AlSi<sub>3</sub>O<sub>8</sub>), PDF:09-0466], Ferrosillite Magnesian [(Mg<sub>0.463</sub>Fe<sub>1.537</sub>)Si<sub>2</sub>O<sub>6</sub>, PDF:88-1917], Forsterite [Mg<sub>2</sub>SiO<sub>4</sub>, PDF:34-0189], Fosterite ferroan [(Mg<sub>0.879</sub>Fe<sub>0.121</sub>)(Mg<sub>0.881</sub>Fe<sub>0.119</sub>)Si<sub>2</sub>O<sub>6</sub>, PDF:83-0645], Hematite [α-Fe<sub>2</sub>O<sub>3</sub>, PDF:89-8103], Maghemite [γ-Fe<sub>2</sub>O<sub>3</sub>, PDF:15-0615], Muscovite 2M<sub>1</sub> [(Na<sub>0.37</sub>K<sub>0.60</sub>)(Al<sub>1.84</sub>Ti<sub>0.02</sub>Fe<sub>0.10</sub>Mg<sub>0.06</sub>)(Si<sub>3.03</sub>Al<sub>0.97</sub>)O<sub>10</sub>(OH)<sub>2</sub>, PDF:82-2452], Nepheline [Na<sub>2</sub>O.Al<sub>2</sub>O<sub>3</sub>.2SiO<sub>2</sub>.1/2H<sub>2</sub>O, PDF :10-0459] and the existence of an amount of amorphous phase characterized by a broad hump found between 20-35° (2θ). Fig.4 presents the FTIR spectrum of MaJ and shows two large absorption regions located from 1649 to 615 cm<sup>-1</sup> and from 4000 to 3000 cm<sup>-1</sup>. The first region shows the peaks of the weak absorption bands located at 615, 683, 747 and 990 cm<sup>-1</sup> which characterize the stretching and bending vibrations of the Si-O-T bonds (T: Si, Al or Fe [17,18,19]. In fact, many authors show that the peaks around 615 cm<sup>-1</sup> can also be attributed to the vibrations of the stretching and bending of the Fe-O bonds of hematite or other iron oxide rich minerals [17,20,21] while that at 747 cm<sup>-1</sup> characterizes the vibration modes of the Si-O bonds of the silicate network [22, 23].

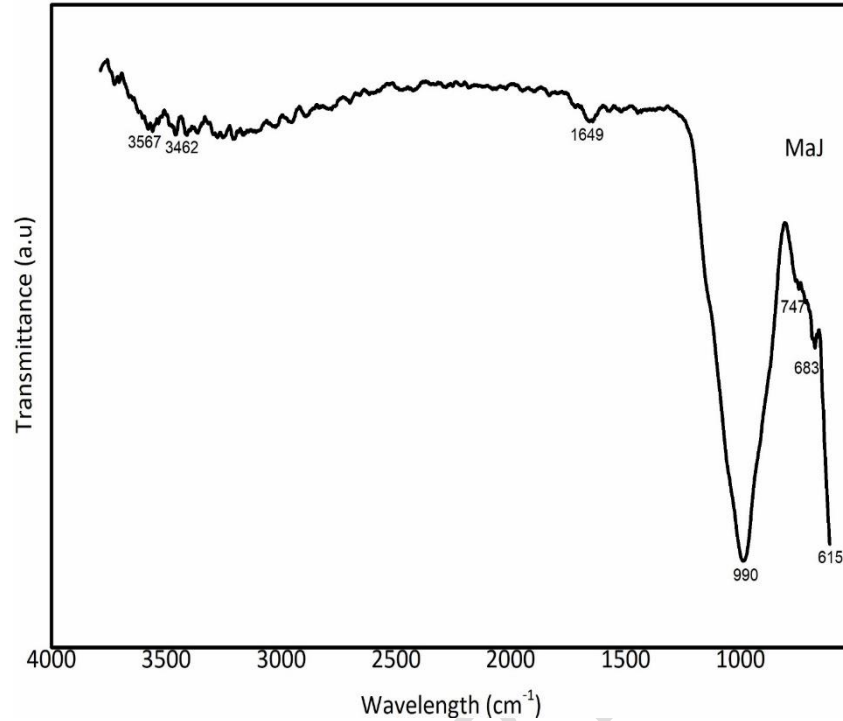


**Fig 4.** IR Spectra of volcanic ash

Additionally, the band at  $990\text{ cm}^{-1}$  is most of time assigned symmetrical bending of the Si-O-T bonds [23], and Fe-O-Si when the solid precursor contains a significant amount of  $\text{Fe}_2\text{O}_3$  [24, 25, 26]. On the other hand, the band located at  $1649\text{ cm}^{-1}$  and around  $3567\text{ cm}^{-1}$  correspond to the vibrations of the O-H and H-O-H bonds of the water molecule respectively. All of these results are in accordance with those of the above XRD and chemical composition of VA.

### ***3.2 Effect of adding of ABCs powder in workability and consistency of the paste***

The different paste prepared by addition of ABC and VA powder required a small amount of acid hardeners (ratio liquid/solid = 0.45) to have a bad workability when the amount of powder ABCs increase. This can be explained by the exothermic reaction which takes place between the diluted phosphoric acid solution used (4M) and the additional aluminum powder from the beverage can. It will therefore be advisable to note that, when the ABCs content increases in the medium, the consistency of the dough and its workability decreases.

### ***3.3. Physicochemical and mechanical properties of porous materials obtained***

#### ***3.3.1. Visual appearance of test tubes and efflorescence***

Fig 5 show the visual appearance of the test pieces of the different formulations and the phenomenon of efflorescence after 28 days of maturity. As regards the visual appearance of the test pieces of the different samples of porous materials obtained, it appears that the more the ABC content increases, the more the formation of small voids is perceptible on the surface of the test pieces. This can be justified by the redox (exothermic) reaction which takes place during the contact between ABCs powder mixed with VA powder and the acid hardener. This reaction takes place with a release of dihydrogen and thus leaving high voids within the material.

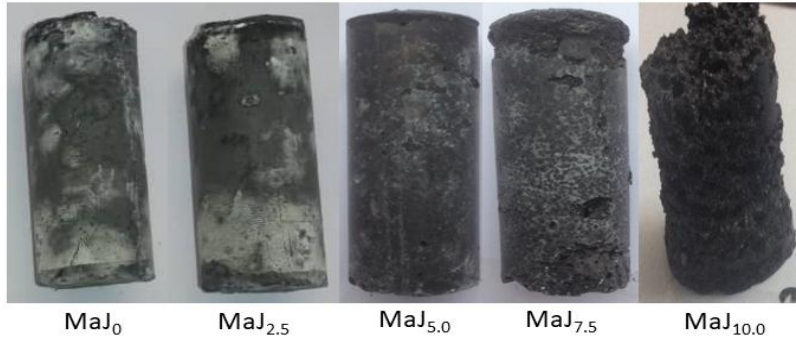


**Fig 5.** Visual appearance and efflorescence of porous polymers aged 28 days

On the other hand, the results of Fig 5 show that the efflorescence phenomenon is perceptible only on the formulation which do not have a substantial ABC content (MaJ<sub>0</sub> and MaJ<sub>2.5</sub>). Indeed, the partial replacement of the powder by a source rich in aluminum leads to the reduction of the phenomenon of efflorescence within synthesized products. Such observations had already been made in several research works [2,27]. Thus, the absence of efflorescence on the other formulations obtained is due to the strong presence of aluminum powder from beverage cans.

### **3.3.2. Apparent porosity and Compressive strength**

The results relating to apparent porosity and compressive strength are recorded in the Table 3 and Fig. 6 and 7 illustrate this graphically. It turns out that the values of the apparent porosity are between 17.2 (MaJ<sub>0</sub>) and 28.1 (MaJ<sub>10</sub>). Thus, it can be seen that the partial replacement of the VA powder by ABCs powder promotes the formation of pores within the material and leads to an increase in the porosity values. In fact, the more the powder of VA is replaced by that of ABC, the more the release of dihydrogen during the attack by the acid solution will be important and the more the size and the volume of the pores will be important on the surface of the material.

**Table 3.** Physical and mechanical characteristics of porous materials

Samples	Bulk density	Apparent	Water	Compressive
---------	--------------	----------	-------	-------------



	(g/cm <sup>3</sup> )	porosity (%)	absorption (%)	strength (MPa)
MaJ <sub>0</sub>	2.56	17.2	20.1	5.90
MaJ <sub>2.5</sub>	1.78	22.6	37.1	2.00
MaJ <sub>5.0</sub>	1.60	26.4	52.0	1.40
MaJ <sub>7.5</sub>	1.43	27.0	52.9	1.20
MaJ <sub>10</sub>	1.32	28.1	54.7	0.80

The images of the cross section of the different specimens observable in Fig. 8 confirm this assertion. This result agrees with the work of other authors who show that adding an additional source of alumina promotes the formation of pores within the material [12].

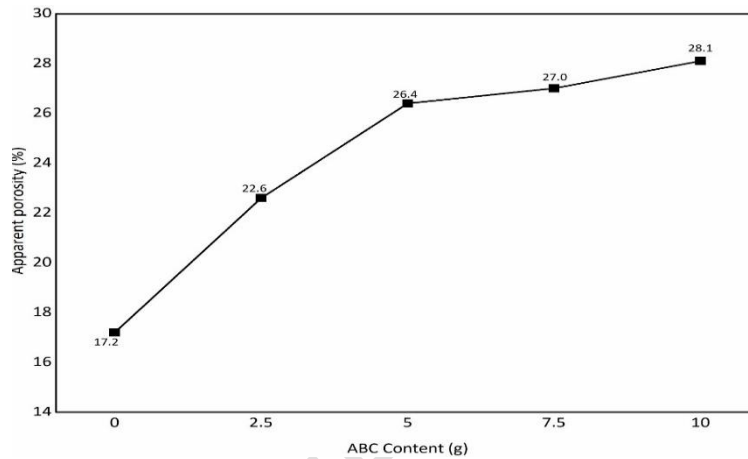


**Fig 6.** Apparent porosity of porous polymers aged 28 days

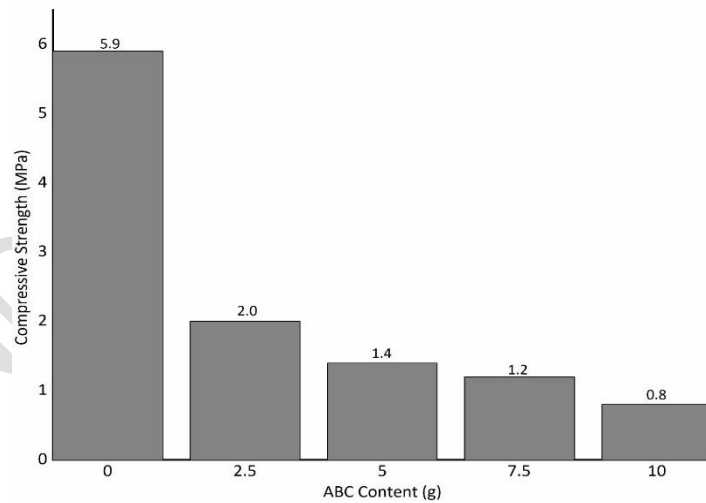


**Fig 7.** Compressive strength of porous polymers aged 28 days

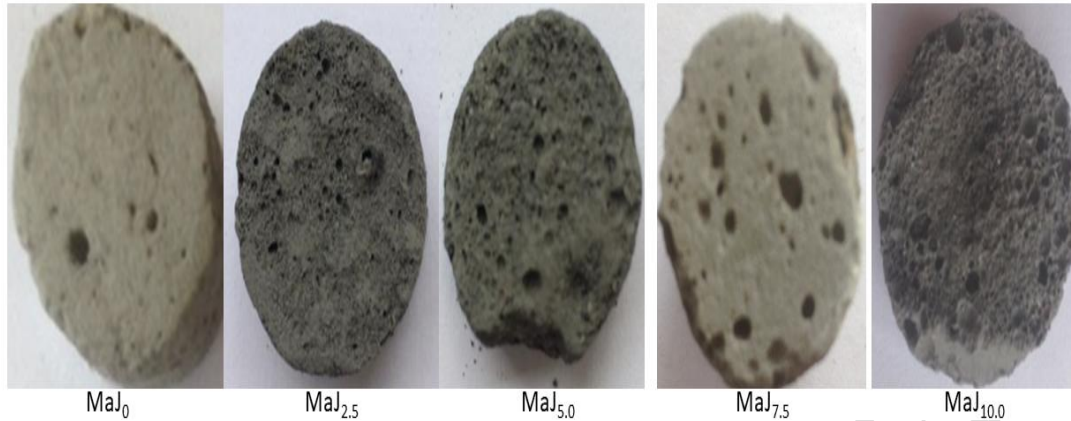


**Fig 8.** Transversal section of porous polymers aged 28 days

Unlike porosity, the compressive strengths of different specimens decrease with increasing ABC content and the values are between 5.9 MPa (MaJ<sub>0</sub>) and 0.8 MPa (MaJ<sub>10</sub>). This result may be justified by the fact that the increase in the ABCs content in the VA powder will promote the formation of voids (pores) within the material upon contact with the acid hardener. It is judicious to note that, the strong presence of voids within a polymer decreases its compactness and promotes the obtainment of low value of compressive strength. Indeed, the exothermic reaction which occurs during contact between the powders (VA/ABC) and the hardener leads to the formation of pores within the material. This will weaken the specimens obtained and consequently cause a reduction in compressive strength. These results are in agreement with those obtained by many authors [12,14] in which he reports that, the more the Al content increases in the final material, the more there will be pore formation and consequently decrease in compressive strength.

### **3.3.3. Bulk density**

The bulk densities ( $\text{g/cm}^3$ ) as function of the replacement level of volcanic ash (0, 2.5, 5.0, 7.5 and 10 by mass) are depicted in Fig. 9. According to this figure, the bulk density of the specimens denoted MaJ<sub>0</sub>, MaJ<sub>2.5</sub>, MaJ<sub>5</sub>, MaJ<sub>7.5</sub> and MaJ<sub>10</sub> are 2.56, 1.78, 1.60, 1.43 and 1.32 respectively. The high density value observed in specimen MaJ<sub>0</sub> ( $2.5 \text{ g/cm}^3$ ) is due to the absence of an additional aluminum source of beverage cans. In other words, the addition of aluminum powder from beverage cans promotes the creation of pores within the polymers obtained when it comes into contact with the hardener. There is a release of dihydrogen and an increase in the temperature of the paste obtained. There is a release of dihydrogen and an increase in the temperature of the paste obtained. This result is in agreement with those observed by Hertel et al [14] which shows that, the addition of higher concentration of aluminum results in the decrease of compressive strength and bulk density. However, during

this exothermic redox reaction, the consistency of the mixture decreases and the probability of reacting all of the VA powder decreases. This will justify the lowering of the different specimens density.

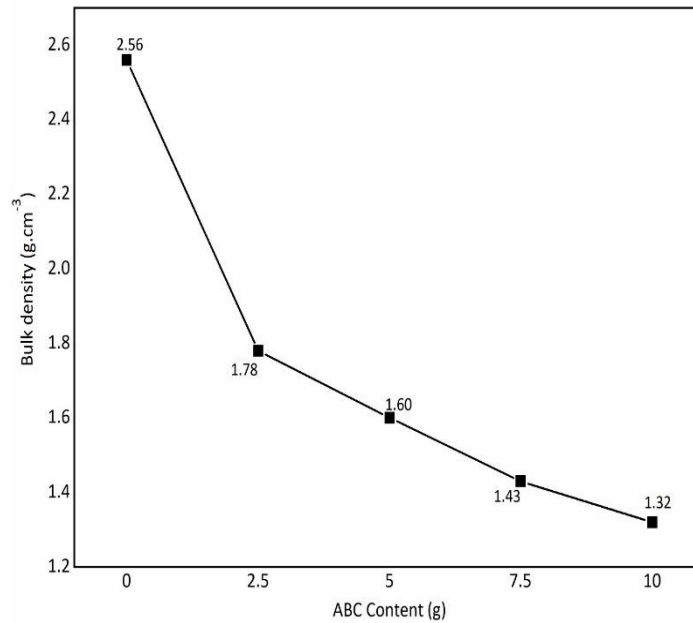


**Fig 9.** Bulk density of porous polymers after 28 days

These results are in agreement with those obtained by other researchers [14,28] reported that the addition of Al powder reduced the bulk density of the final specimens in the synthesis of porous inorganic polymers.

#### **3.3.4. Water absorption**

The percentage of water absorption is a function of the partial replacement of the volcanic ash (0, 2.5, 5.0, 7.5 and 10 by mass) illustrated in Fig. 10. It appears that the water absorption of MaJ<sub>0</sub>, MaJ<sub>2.5</sub>, MaJ<sub>5</sub>, MaJ<sub>7.5</sub> and MaJ<sub>10</sub> are 20.1, 37.1, 52.0, 52.9 and 54 % respectively. Unlike density and compressive strength, the values of water absorption increases with the addition of ABCs powder. The increase in this value of the percentage of water absorption with an increase in the ABC powder shows that the latter can be used as a blowing agent during the synthesis of inorganic phosphate polymers. Furthermore, Fig 8. highlights the cross section of the different specimens obtained, it shows that the size and volume of the cavities observed increases with the ABC contents. This then justifies the high retention capacity of the water molecules during the absorption test.

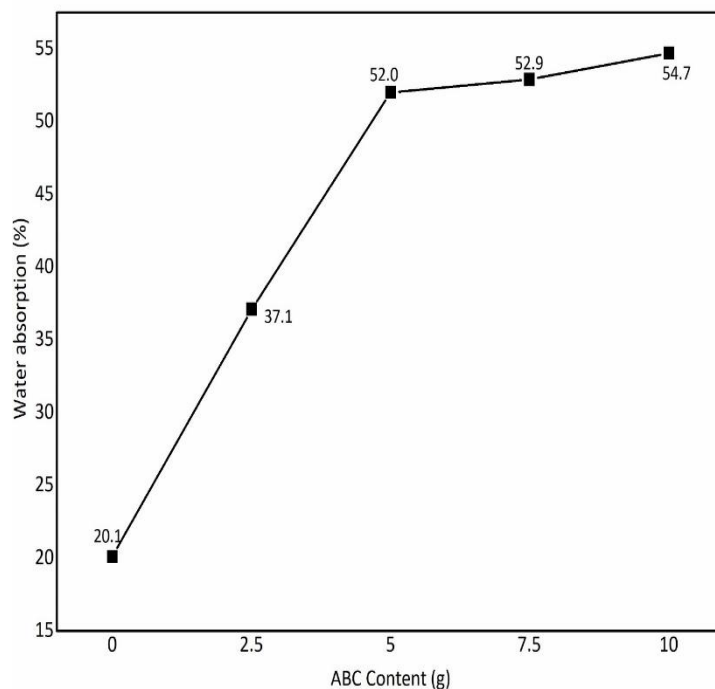


**Fig 10.** Water absorption of porous material aged 28 days

#### 4. CONCLUSION

This study consisted of evaluating the physical and mechanical properties of porous materials obtained from the partial replacement of volcanic ash powder by that of aluminum beverage cans. The results obtained show that:

- Increase in ABC content during the synthesis of porous materials increases the consistency of the dough and reduces its workability ;
- The formations of pores within the material, the porosity and the water absorption increase with the aluminum beverage cans contents, while the phenomenon decreases ;
- The compressive strength and apparent density of the porous materials obtained decreases with the increase in ABC content ;
- This work shows that the aluminum beverage cans to be able revalued and used as a blowing agent during the synthesis of porous inorganic polymers.

However, it would be wise in the long run to determine the mineralogical, microstructural and toxicological characteristics of the different polymers obtained in order to better orient their fields of application.

## REFERENCES

- [1] Kamseu, E.; Leonilli, C.; Perera, D. S.; Melo, U. C.; Lelougna, P. N. Investigation of the volcanic ash based cement as potential building materials. *Inter Ceram Int.* 2000, 58, 136-140.
- [2] Djobo, J. N. Y.; Elimbi, A.; Tchakouté, H. K.; Kumar, S. Volcanic ash-based geopolymers cements/concretes :The current state of the art and perspectives. *Environ Sci Pollut Res.* 2017, 24, 4433-4446.
- [3] Baenla, J.; Bike, J. B. M.; Djon Li Ndjock, I. B.; Elimbi, A. Partial replacement of low reactive volcanic ash by cassava pell ash in synthesis of volcanic ash based geopolymers. *Constr Build Mater.* 2019, 227,116689.
- [4] Djon Li Ndjock, I. B.; Baenla, J.; Bike, J. B. M.; Elimbi, A.; Cyr,M. Amorphous phase of volcanic ash and microstructure of cement product obtained from phosphoric acid activation. *SN Applied Sciences.* 2020, 2,720.
- [5] Djon Li Ndjock, I. B.; Elimbi, A.; Cyr,M. Rational utilization of volcanic ashes based on factors affecting their alkaline activation. *J Non-Cryst Solids.* 2017, 463, 31-39.
- [6] Kawamoto, K.; Moldrup, P.; Komatsu, T.; Wollesen de Jonge, L.; Oda, M. Water repellency of aggregate size fraction of a volcanic ash soil. *Soil Science Society of America Journal.* 2007, 71(6), 1658-1666.
- [7] Agence Ecofin. Available online: <https://www.agenceecofin.com/agro/2802-54793-apres-les-...-conditionnement-des-boissons-gazeuses-dans-les-canettes> (29/06/2020).
- [8] Regional reports.<http://recycling.world-aluminium.org/regional-reports/brazil/>
- [9] Madehow. Available online: <http://www.madehow.com/Volume-2/Aluminum-Beverage-Can.html> (29/06/2020).
- [10] Kamseu, E.; Nait- Ali, B.; Bignozzi, M. C.; Leonilli, C.; Rossignol, S.; Smith, D.S. Bulk composition and microstructure dependence of effective thermal conductivity of porous inorganic polymer cements. *Jeurceramsoc.* 2012, 32, 1593-1603.
- [11] Prud'homme, E.; Michaud, P.; Joussein, E.; Peyratout, C.; Smith, A.; Arrii- Clacens, S.; Clacens, J. M.; Rossignol, S. Silica fume as porogent agent in geo-materials at low temperature. *Jeurceramsoc.* 2010, 30, 1641-1648.
- [12] Le-ping, L.; Xue-min, C.; Shu-heng, Q.; Jun-li, Y.; Zhang Lin. Preparation of phosphoric acid-based porous geopolymers. *Appl. Clay Sci.* 2010, 50, 600-603.
- [13] Al-Saidi, H.M.; Farghaly, O.A.; El-Sayed, M.E.A.; Abd-Elmottaleb, M.; Elmaghraby, T.A.; Ahmed, M.G.Z. Efect of Al & Fe inorganic polymers on the enhancement of the surface properties activated carbon prepared from sesame stalks. *Life Science Journal.* 2020, 17(1).

- [14] Hertel, T.; Novais, R. M.; Alarcon, R.M.; Labrincha, J.A.; Pontikes, Y. Use of modified bauxite residue-based porous inorganic polymer monoliths as adsorbents methylene blue. *J. Clean Prod.* 2019, 227,877-889.
- [15] ASTM C 20-00. Standard test methods for apparent porosity, water absorption, apparent specific gravity and bulk density of burned refractory brick and shapes by boiling water. 2010. pp. 1-3.
- [16] Davidovits, J. Geopolymers: Ceramic-Like Inorganic Polymers. *J. Ceram. Sci. Technol.* 2017, 8(3), 335-350.
- [17] Nkwaju, R. J.; Djobo, J. N. Y.; Nouping, J. N. F.; Huisken, P. W. M.; Detou, J. G. N.; Couard, L. Iron- rich laterite- bagasse fibers geopolymers composites: Mechanical, durability and insulating properties. *Appl. Clay Sci.* 2019, 18, 105333.
- [18] Kaze, R. C.; Beuleuk à Mougam, L.M.; Fonkwe, M. L. D.; Nana, A.; Kamseu, E.; Melo, U. F. C.; Leonelli, C. The corrosion of kaolinite by iron minerals and the effects on geopolymerization. *Appl. Clay Sci.* 2017, 138, 48-62.
- [19] Louati, S.; Baklouti, S.; Samet, B. Geopolymers based on phosphoric acid and illito-kaolinitic clays. *Adv Mater Sci Eng.* 2016, <http://doi.org/10.1155/2016/2359759>.
- [20] Khabbouchi, M.; Hosni, K., Srasra, E. Physico- chemical characterization of modified Tunisian kaolin by phosphoric acid. *Surf. Engin Appl.Electrochem.* 2018, 54, 219-226.
- [21] Legodi, M.A.; De wall, D. The preparation of magnetite, goethite, hematite and maghemite of pigment quality from mill scale iron waste. *Dyes and Pigments.* 2007, 74, 161-168.
- [22] Djobo, J. N. Y.; Elimbi, A.; Tchakouté, H. K.; Kumar, S. Reactivity of volcanic ash in alkaline medium, microstructural and strength characteristics of resulting geopolymers under different synthesis conditions. *J. Mater. Sci.* 2016, 51, 10301-10317.
- [23] Bewa, C. N.; Tchakouté, H. K.; Ruscher, C. H.; Kamseu, E.; Leonelli, C. Influence of the curing temperature on the properties of poly (phospho- ferro- siloxo) networks from laterite. *SN Applied Sciences.* 2019, 1, 916.
- [24] Kaze, R. C.; Beuleuk à Mougam, L.M.; Rosa, R.; Kamseu, E.; Melo, U.C.; Leonelli, C. Microstructure and engineering properties of Fe<sub>2</sub>O<sub>3</sub> (FeO)-Al<sub>2</sub>O<sub>3</sub>-SiO<sub>2</sub> based geopolymers composites. *J. Clean Prod.* 2018, 199, 849-859.
- [25] Vempati, R. K.; and Loeppert, R.H. Influence of Structural and Adsorbed Si on the Transformation of synthetic Ferrihydrite, *Clays and Clay Miner.* 1989, 37(3) 273-279.
- [26] Gallup, L. D.; Reiff, W. M. Characterization of Geothermal Scale Deposits by Fe-57 Mossbauer Spectroscopy and Complementary X-Ray Diffraction and Infrared Studies. *Gethermics.* 1991, 20(4), 207-224.

[27] Djobo, J. N. Y.; Elimbi, A.; Dika, M. J.; Djon Li Ndjock, I. B. Partial replacement of volcanic ash by bauxite and calcined oyster shell in synthesis of volcanic ash-based geopolymers. *Constr.Build.Mater.* 2016,113, 673-681.

[28] Chaipanich, A.; Chindapasirt, P. The properties and durability of autoclaved aerated concrete masonry blocks. *Eco- efficient Masonry Bricks and Blocks*, Pacheco- Torgal, F., Lourenço, P. B., Labrincha, J., Chindapasirt, P., Kumar, S.; Publisher: Woodhead publishing, Thailand, 2015; pp. 215-230.

UNDER PEER REVIEW